Angewandte Chemie
Eine Zeitschrift der Gesellschaft Deutscher Chemiker

Supporting Information

© Wiley-VCH 2008

69451 Weinheim, Germany

Combined Quasi-Elastic Neutron Scattering and Molecular Dynamics Study of Methane Diffusion in Metal Organic Frameworks MIL-47(V) and MIL-53(Cr), N. Rosenbach Jr., H. Jobic*, A. Ghoufi, F. Salles, G. Maurin*, S. Bourrelly, P.L. Llewellyn, T. Devic, C. Serre & G. Férey.

Supporting information

Charge distributions

A periodic model of both the MIL-47(V) and the MIL-53 (Cr) materials was first geometry optimised, using the crystallographic coordinates of the atoms as starting configurations.[1,2]. Since the positions of the H atoms cannot be detected by X-Ray Diffraction, these atoms were added to the organic groups and to the μ_2 position, using the H-adding facility in the Cerius Visualiser software[3]. For the inorganic moiety, this means that hydrogen atoms were added to the phenyl rings, keeping consistent with well-established C—H bond lengths (1.14 Å) and C—C—H angles (120°). For the inorganic part, the hydrogen atoms were included such that the O—H bonds were perpendicular to the M—O—M linkages and the bond lengths were set at 0.95 Å The partial charges for the hybrid porous systems were then extracted using periodic Density Functional Theory calculations and Mulliken charge partitioning method as previously reported.[4] The Accelrys DMol[3] code was used for these calculations which were performed using the PW91 GGA density functional, and the double numerical basis set containing polarisation functions on hydrogen atoms (DNP).[5] The resulting charges carried by all the atoms are reported in Table S1, the position of each atom type on the framework being shown in Figure S1.

We have recently shown that these charges only slightly differ from those extracted using a cluster approach combined to the electrostatic potential derived method CHELPG[6]; they are very similar for the organic linkers and only slightly deviate for the metal center atoms (Cr and V). The Mulliken scheme was selected as the microscopic model to describe CH_4 was initially built using charges determined by this method[7]. In that model, the CH_4 molecule was represented by an atomic point charge model with the following partial charges (in electron units): C (-0.472) and H (+0.118).

Atoms	h_c	cg1	cg2	C_c	o_c	M	μ_2_o	h_o
Charges MIL-47(V)	0.146	-0.071	-0.068	0.604	-0.496	1.207	-0.596	
Charges MIL-53(Cr)	0.139	-0.074	-0.074	0.613	-0.506	1.031	-0.637	0.291

Table S1: Atomic partial charges (in electron units) carried by the different atoms within the MIL-47(V) and MIL-53(Cr) frameworks, the labels of the atoms are described in Figure S1.

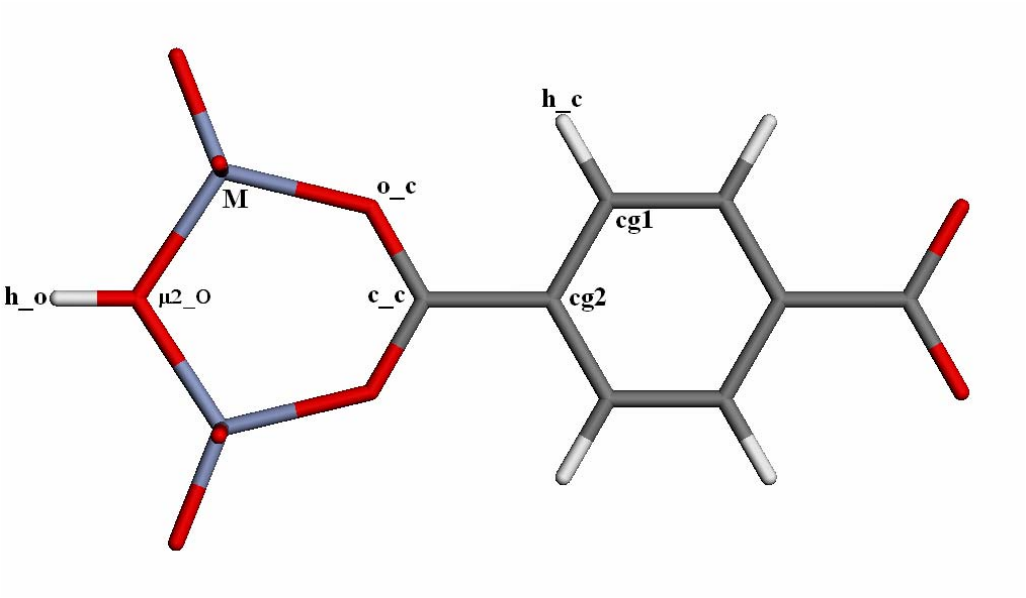

Figure S1 - Labels of the atoms for the organic and inorganic parts for both MIL-53 (Cr) and MIL-47 (V) materials corresponding to the forcefield atom types, to allow the easy reading of Tables S1 and S2.

Interatomic potentials

CH_4 was represented by a 5-point charge model where each atom provides a contribution to the adsorbate/adsorbate and adsorbate/adsorbent interactions which are described via a repulsion-dispersion 12-6 Lennard Jones (LJ) potential and a Coulombic term. The CH_4 molecule was defined with a well defined distance of d(C-H) = 1.10 Å. The CH_4/CH_4 LJ parameters, were taken from our previous investigations.[7] For the interaction between CH_4 and the organic moiety of both MIL frameworks, the parameters of CH_4 were combined with that taken from the widely used Dreiding force field[8], using

Lorentz–Berthelot mixing rules, to obtain the new set of cross interatomic pair potential parameters. Further, the dispersion-repulsion interactions between the CH_4 molecules and the metal centers of the inorganic part (Cr(OH) and V(O)) were not taken in account, as the polarisabilities of these centers are much lower than those of the oxygen atoms. Indeed, the repulsion-dispersion contribution of the inorganic part was assigned only to the oxygen atoms as well as the protons of the μ_2-OH groups in the case of the MIL-53 (Cr) material.[7] The corresponding LJ parameters to describe the interactions between CH_4 and the oxygen atoms were extracted from our previous *ab initio* derived forcefields which successfully reproduced the CH_4 adsorption properties in purely siliceous zeolite materials[7]. In addition, the interaction between CH_4 and the protons was modelled by a Buckingham potential whose parameters were taken from our recent studies on the CH_4 adsorption in STA-7 SAPO material[9]. These set of potential parameters were derived using the same quantum cluster approach we reported for representing the interaction between the proton of a SAPO material and CO_2.[10]

All the interatomic potential parameters are listed in Table S2.

(a) Nonbonded Lennard-Jones potentials

Atom pairs	**σ (Å)**	**ε (eV)**
c_m/c_m	3.473	0.00309
h_m/h_m	2.846	0.00066
c_m/h_m	3.293	0.00136
c_m/h_c	3.160	0.00143
h_m/h_c	2.846	0.00066
c_m/cg1, c_m/cg2 and c_m/c_c	3.473	0.00357
h_m/cg1, h_m/cg2 and h_m/c_c	3.160	0.00165
c_m/o_c and c_m/μ_2_o	3.200	0.00599
h_m/o_c and h_m/μ_2_o	2.899	0.00362

(b) Nonbonded Buckingham potentials

Atom pairs	**ρ (Å)**	***A* (eV)**	***C* (eV)**
c_m/h_o	3.950	1020.41055	20.86350
h_m/h_o	3.860	35.35799	0.00000

(c) Bonded potentials

Type	**r_{eq} (Å) or θ_{eq} (°)**	**K_r (eV Å^{-2}) or K_θ (eV rad^{-2})**
c_m/h_m stretching	1.095	28.71094
h_m-c_m-h_m bending	109.2	2.05970

Table S2 – Interatomic pair potential parameters for both CH_4/CH_4 and CH_4/hybrid porous framework used in the GCMC and MD simulations.

Grand Canonical Monte Carlo simulations

Absolute adsorption isotherms for both MILs were computed up to 30 bar using a Grand Canonical Monte Carlo algorithm, as implemented in the Sorption module of the Cerius[2] software suite[3]. We performed all the simulations at 303 K with a simulation box corresponding to 16 unit cells with typically 2.5×10^6 Monte Carlo steps. The framework was kept rigid during the whole adsorption process, considering the bare DFT optimised structures which are very similar to those extracted by X-ray Diffraction. This assumption is justified by previous *in situ* X-ray diffraction data collected on both MIL-47(V) and MIL-53(Cr) upon CH_4 adsorption which showed that the cell parameters of the structure remain unchanged up to high pressure.[11] The Ewald summation was used for calculating electrostatic interactions and the short range interactions were computed with a cut-off distance of 12 Å. The differential adsorption enthalpy at low coverage was calculated through the fluctuation over the number of particles in the system and from the internal energy.

Figures S2a and S2b report the simulated absolute isotherms for CH_4 adsorption on both the MIL-47 (V) and the MIL-53 (Cr) at 303 K and up to 30 bar which are compared to those extracted by microcalorimetry on the deuterated samples used for the QENS measurements. As the adsorbate slightly deviates from ideal gas behaviour in the whole range of pressure, the simulated data were corrected through an experimental equation of state to take into account this non-ideal state. We observe that the simulated absolute isotherms fairly reproduce the experiments for both MIL-47(V) and MIL-53(Cr) in the whole range of pressure while they only slightly underestimate the experimental adsorbed amounts at low pressure. This good agreement experiment-simulation shows that the CH_4/CH_4 and CH_4/MIL framework force fields are reliable to describe the interactions within the whole system. Further, it means that both investigated MIL samples are of good quality with an efficient activation process, as we know that molecular simulations are carried out in perfect and infinite crystals. Another way to validate the different force fields consists of comparing the calculated and the experimental enthalpies which are related to a direct measurement of the strength of the interaction between the adsorbate and the adsorbent surface. In that way, we get a very good agreement between the experimental and simulated differential

enthalpies of adsorption at low coverage in both MIL-47(V) (15.9 kJ.mol^{-1} vs 15.6 kJ.mol^{-1}) and MIL-53(Cr) (18.0 kJ.mol^{-1} vs 17.9 kJ.mol^{-1}).

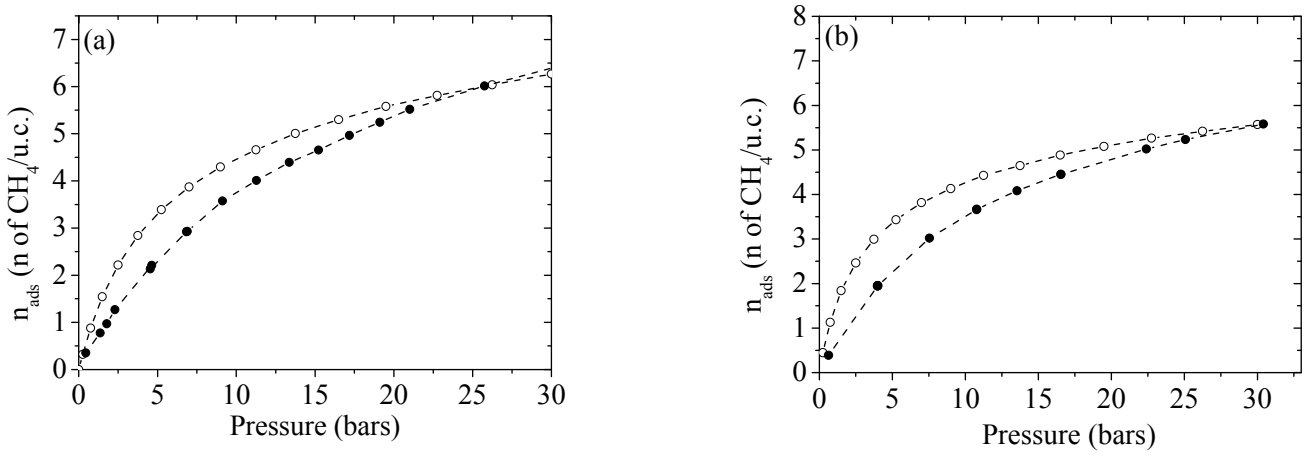

Figure S2 – Absolute adsorption isotherms as a function of the pressure for CH_4 adsorbed in both (a) MIL47(V) and (b) MIL53(Cr): (●) experiment and (○) simulation.

Figures S3a and S3b report typical arrangements of CH_4 molecules within the pore of both MIL materials, for an intermediate loading. MIL-47(V) (Figure S3a) does not exhibit any preferential adsorption sites, the CH_4 molecules being homogeneously distributed within the pore, with characteristic distances separating the hydrogen of the CH_4 molecule and both the organic and inorganic parts of the framework ranged from 3.2 to 3.8 Å. This result is consistent with the analogous behaviour observed for the adsorption of CH_4 in purely siliceous zeolites such as silicalite or DAY.[12] For MIL-53(Cr) (Figure S3b), the CH_4 tends to be more localized, preferentially interacting with the hydroxyl groups at the surface. As the distances between the adsorbate and the MIL framework become shorter than those observed for MIL-47(V), it explains the higher enthalpy for MIL-53(Cr).

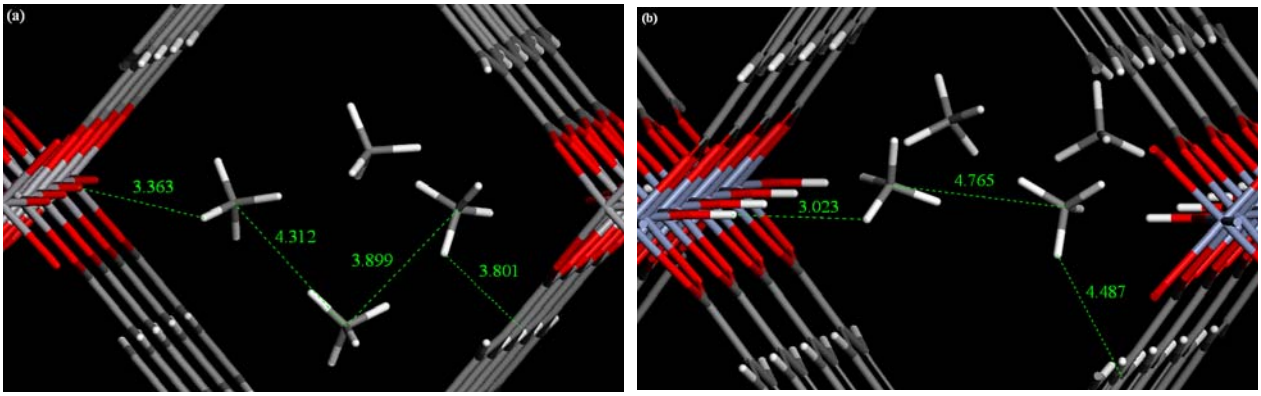

Figure S3 – A typical illustration of the CH_4 arrangement in the (a) MIL-47(V) and (b) MIL-53(Cr) structure at low corresponding to 2 molecules per unit cell. The reported distances are in Å.

Molecular Dynamics simulations

Molecular dynamics simulations were performed using the DL_POLY program[13] in the NVT ensemble and the Evans isokinetic thermostat.[14] The MIL framework was maintained fixed during the simulations. By contrast, CH_4 was treated as fully flexible as it is well known that this parameter can significantly influence the diffusivity behaviour in nanoporous materials. The flexibility of this adsorbate was described by two-body bond and three-body angle potentials using the parameters taken from Oie *et al.*[15] (Table S2). We selected for each investigated loading, the structures obtained by Grand Canonical Monte Carlo (GCMC) simulations as starting configurations and the minimised cell dimensions were kept fixed during the MD runs. For both MILs, the calculations were performed at 250K, for 0,5, 1, 2, 3 and 5 CH_4 molecules/u.c., i.e. 8, 16, 32, 48 and 80 molecules in the simulation box respectively, to be consistent with the experimental loading. Each run was realised for 2. 10^6 steps (i.e. 2 ns) with a time step of 1 fs, following 0.5 ns of equilibration. The configurations were stored every 200 time steps.

In order to evaluate the activation energies corresponding to the self-diffusion process, additional simulations were performed for 2 molecules/u.c. in a range of temperatures between 250 and 400 K. The mean square displacements (MSDs) for the CH_4 molecules for each loading and at the different temperatures were evaluated by means of the following classical equation:

$$\mathrm{MSD}(t) = \left\langle \Delta r_j^2(t) \right\rangle = \frac{1}{N}\sum_{j=1}^{N} \Delta r_j^2 = \frac{1}{N}\sum_{j=1}^{N} [r_j(t) - r_j(0)]^2$$

where N corresponds to the number of methane molecules considered in the computation of the MSD. In order to improve the statistics of the calculation, 5 MD trajectories were sampled for each loading and we used multiple time origins as described elsewhere.[14] Each trajectory was generated for both MILs by starting with different initial arrangements of CH_4 within the tunnel created by additional Canonical Monte Carlo simulations. Figure S4 reports the global MSD curves in MIL-47(V) averaged over the 5 MD trajectories and over multiple time origins. They are very similar to the MSD calculated along the z direction as the contributions along the x and y axis are negligible. We can notice, at all loading, that the MSDs present a profile reasonably linear from 200 ps and over a broad time domain which corresponds to the diffusion regime. The self diffusivities (D_s) were then evaluated by fitting the MSDs plots as a function of the time in the region 200-500 ps, assuming the Einstein's relation. This procedure is consistent with that proposed by Chitra and Yashonath[16] who suggested to consider lower and upper times in such a way to avoid both the initial (ballistic regime) and the long (poor statistics due to less data points) time regions. An approximate value of the statistical error of D_s was calculated from the standard deviation from the 5 MD trajectories.

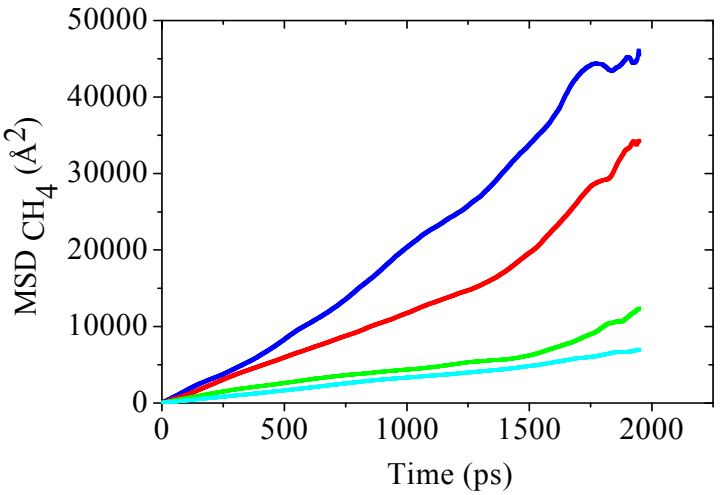

Figure S4 – MSD curves for CH_4 at 250 K in MIL-47(V) averaged from multiple time origins and 5 different MD trajectories (1 CH_4/u.c. : blue, 2 CH_4/u.c.: red, 3 CH_4/u.c.: green and 5 CH_4/u.c.: cyan).

The activation energies corresponding to the self-diffusion processes were evaluated from the linear least-squares fit to the Arrhenius plots of $\ln(D_s) = f(1000/T)$.

The 2D free-energy maps were then obtained using the histogram sampling (HS) method previously reported by Beerdsen et al[17]. From the probability density plot labelled P(S) (illustration in Figure 5 reported at low loading), a 2D free energy map (F(S)) is calculated using the following equation :

$$\beta F(S) = -\ln\langle P(S)\rangle$$

where β=kT with k, the Boltzmann constant

Using the trajectories recorded during our MD runs, the mean residence time of CH_4 around the μ_2-OH (in MIL-53(Cr) and the μ_2-O (in MIL-47(V) groups, has been estimated at low loading from the correlation function r(t) defined by the following equation[18]:

$$r(t) = \frac{\left\langle P_j(t, t_i, t^*)\right\rangle_j}{\left\langle P_j(0, t_i, t^*)\right\rangle}$$

where $P_j(t, t_i, t^*)$ is the Heaviside unit step function equals to 1 if the methane molecule j is present in the region delimited by a sphere centred on the oxygen of the μ_2-OH groups in MIL-53(Cr) (μ_2-O in MIL-47(V) of 5 Å radius, at both time t_i and $t_i + t$. Otherwise, the unit step function equals zero. The parameter t* takes into account methane molecules which leave the delimited region temporarily, but for a time period shorter than t^*. As we were interested to compare the relative values between MIL-47(V) and MIL-53(Cr), we selected different t^* value and we showed that the difference of residence times is not significantly affected by this arbitrary choice.

The r(t) function has been thus fitted using the second order exponential decay as previously reported[19] :

$$r(t) = A_1 \exp\left(-\frac{t}{\tau_1}\right) + A_2 \exp\left(-\frac{t}{\tau_2}\right)\}$$

where τ_2 corresponds to the residence time of the CH_4 molecules around the μ_2-OH (in MIL-53(Cr) or the

μ_2-O (in MIL-47(V)) groups.

In figure S5, the τ_2 values are reported in MIL-47(V) and MIL-53(Cr) for a loading of 2 CH_4/u.c., as a function of t^*. It is clearly shown that the mean residence times remains always significantly higher in MIL-53(Cr) whatever the value considered for t^*. The mean values are 5.4 ps and 3.3 ps in MIL-53(Cr) and MIL-47(V) respectively for a t^* value of 0.5 ps.

Figure S5 : Mean residence times τ_2 obtained for MIL-53(Cr) (empty symbols) and MIL-47(V) (full symbols) as a function of the considered value for t^* for a loading of 3 CH_4 molecules/u.c..

References

C. Serre, F. Millange, C. Thouvenot, M. Nogués, G. Marsolier, D. Louer, G. Férey, *J. Am. Chem. Soc*., **2002**, 124, 13519.

K. Barthelet, J. Marrot, D. Riou, G. Férey, *Angew. Chem., Int. Ed*. **2002**, 41, 281,

Cerius^2. v. 4.0, Accelrys Inc., San Diego, **1999**.

N.A. Ramsahye, G. Maurin, S. Bourrelly, P.L. Llewellyn, T. Loiseau, G. Férey, *Phys. Chem. Chem. Phys*. **2007**, 9, 1059.

Dmol^3. Accelrys Inc., San Diego, **1999**.

G. Festa, N. Ramsahye, S. Bourrelly, P.L. Llewellyn, C. Serre, Th. Devic. G. Férey, G. Maurin, T. Düren, Manuscript in preparation.

G. Maurin, P.L. Llewellyn, R. Bell, *Micropor. Mesopor. Mater*. **2006**, 89, 96.

S.L. Mayo, B.D. Olafson, W.A. Goddard III, *J. Phys. Chem*. **1990**, 94, 8897.

I. Déroche *et al*, Manuscript in preparation.

I. Déroche, L. Gaberova, G. Maurin, M. Castro, P.W. Wright, P.L Llewellyn, P. *J. Phys. Chem. C*, **2008**, 112, 5048.

P.L. Llewellyn, G. Maurin, Th. Devic, S. Loera, N. Rosenbach, C. Serre, S. Bourrelly, P. Horcajada, G. Férey, *J. Am. Chem. Soc*., **submitted**.

J.A. Dunne, M. Rao, S. Sircar, R.J. Gorte, A.L. Myers, *Langmuir*, **1996**, 12, 5896.

W. Smith, T.R. Forester*, J. Mol. Graph.* **1996**, 14, 136.

D. Frenkel, B. Smit, *Understanding Molecular Simulation*; Academic Press: San Diego, CA, **1996**.

T. Oie, T.M. Maggiora, R.E. Christoffersen, D.J. Duchamp, *Int. J. Quantum Chem. Quantum Biol. Symp*. **1981**, 8, 1.

R. Chitra, S. Yashonath, *J. Phys. Chem. B*, **1997**, 101, 5437.

E. Beerdsen, B. Smit, D. Dubbeldam, *Phys. Rev. Lett*., **2004**, 93, 248301.

A.P. Lyubartsev, A. Laaksonen, *J. Phys. Chem*., **1996**, 100, 16410.

F. Goujon, P. Malfreyt, J.M. Simon, A. Boutin, B. Rousseau, A.H. Fuchs, *J. Chem. Phys*., **2004**, 121, 24